



Published in final edited form as:

*J Mol Cell Cardiol.* 2018 March ; 116: 106–114. doi:10.1016/j.yjmcc.2018.01.017.

## Decreased ATP production and myocardial contractile reserve in metabolic heart disease

Ivan Luptak<sup>a</sup>, Aaron L. Sverdlov<sup>a,d</sup>, Marcello Panagia<sup>a</sup>, Fuzhong Qin<sup>a</sup>, David R. Pimentel<sup>a</sup>, Dominique Croteau<sup>a</sup>, Deborah A. Siwik<sup>a</sup>, Joanne S. Ingwall<sup>c</sup>, Markus M. Bachschmid<sup>b</sup>, James A. Balschi<sup>c</sup>, Wilson S. Colucci<sup>a,\*</sup>

<sup>a</sup>Myocardial Biology Unit, Boston University School of Medicine, Boston, MA, United States

<sup>b</sup>Vascular Biology Unit, Boston University School of Medicine, Boston, MA, United States

<sup>c</sup>Physiological NMR Core Laboratory, Brigham and Women's Hospital, Harvard Medical School, Boston, MA, United States

<sup>d</sup>Heart Failure Unit, School of Medicine and Public Health, University of Newcastle, NSW 2300, Australia

### Abstract

Metabolic syndrome is a cluster of obesity-related metabolic abnormalities that lead to metabolic heart disease (MHD) with left ventricular pump dysfunction. Although MHD is thought to be associated with myocardial energetic deficiency, two key questions have not been answered. First, it is not known whether there is a sufficient energy deficit to contribute to pump dysfunction. Second, the basis for the energy deficit is not clear. To address these questions, mice were fed a high fat, high sucrose (HFHS) 'Western' diet to recapitulate the MHD phenotype. In isolated beating hearts, we used <sup>31</sup>P NMR spectroscopy with magnetization transfer to determine a) the concentrations of high energy phosphates ([ATP], [ADP], [PCr]), b) the free energy of ATP hydrolysis ( $G_{-ATP}$ ), c) the rate of ATP production and d) flux through the creatine kinase (CK) reaction. At the lowest workload, the diastolic pressure-volume relationship was shifted upward in HFHS hearts, indicative of diastolic dysfunction, whereas systolic function was preserved. At this workload, the rate of ATP synthesis was decreased in HFHS hearts, and was associated with decreases in both [PCr] and  $G_{-ATP}$ . Higher work demands unmasked<sup>d</sup> the inability of HFHS hearts to increase systolic function and led to a further decrease in  $G_{-ATP}$  to a level that is not sufficient to maintain normal function of sarcoplasmic  $Ca^{2+}$ -ATPase (SERCA). While [ATP] was preserved at all work demands in HFHS hearts, the progressive increase in [ADP] led to a decrease in  $G_{-ATP}$  with increased work demands. Surprisingly, CK flux, CK activity and total creatine were normal in HFHS hearts. These findings differ from dilated cardiomyopathy, in which the energetic deficiency is associated with decreases in CK flux, CK activity and total creatine. Thus, in HFHS-fed mice with MHD there is a distinct metabolic phenotype of the heart characterized

This is an open access article under the CC BY-NC-ND license (<http://creativecommons.org/licenses/by-nc-nd/4.0/>).

\*Corresponding author at: Cardiovascular Medicine Section, Boston University Medical Center, 88 E Newton St, Boston, MA 02118, United States. wilson.colucci@bmc.org (W.S. Colucci).

### Appendix A. Supplementary data

Supplementary data to this article can be found online at <https://doi.org/10.1016/j.yjmcc.2018.01.017>.

by a decrease in ATP production that leads to a functionally-important energetic deficiency and an elevation of [ADP], with preservation of CK flux.

## Keywords

Metabolism; Contractile function; Obesity; Metabolic syndrome; Heart failure

---

## 1. Introduction

The United States is in the midst of an obesity epidemic [1]. More than one third of Americans have metabolic syndrome, a cluster of obesity-related metabolic abnormalities including type 2 diabetes, hypertension, elevated triglycerides and/or decreased HDL cholesterol [2]. Patients with metabolic syndrome have an increased risk of subclinical cardiac dysfunction, referred to here as metabolic heart disease (MHD), that is characterized by left ventricular (LV) hypertrophy and diastolic dysfunction [3-5]. These patients typically have normal resting systolic function as reflected by a normal LV ejection fraction, and may be asymptomatic or progress to clinical heart failure, typically with a preserved ejection fraction (i.e., HFpEF) [6,7].

Studies in humans with obesity-related MHD have shown a decrease in the concentration of myocardial phosphocreatine (PCr), thereby supporting the suggestion that there is an imbalance in energy supply and demand [8]. This thesis is further supported by observations in genetic or diet-induced models of MHD showing an impaired metabolic efficiency in working hearts [9]. Likewise, we [10,11] and others [12,13] have shown that maximal ATP production is decreased in isolated cardiac mitochondria from mice or rats with diet-induced MHD. However, there are at least two important limitations to our current understanding of energetics in MHD. First, the basis for the energy deficit in terms of high energy phosphate fluxes is not clear. Second, it is not clear whether the proposed energy deficit is sufficient to result in a decrease in cardiac pump function. In this study we tested the hypotheses that MHD a) causes a decrease in myocardial ATP synthesis in the intact beating heart, and b) that the resulting decrease in myocardial energy supply is sufficient to depress cardiac function, particularly, in the face of increased work demand.

MHD was caused by feeding mice a high fat, high sucrose, (HFHS) “Western” diet for 4 months [10,14]. Myocardial function was measured in the isolated perfused beating heart, and myocardial energetics were assessed using  $^{31}\text{P}$  NMR spectroscopy [15-17]. To determine the relationship between myocardial energetics and function, we measured contractile function and high energy phosphates simultaneously over a range of workloads. Myocardial [ATP], [ADP] and [PCr] were determined. The severity of the energetic deficit was quantitated by determining the free energy of ATP hydrolysis ( $G_{\sim\text{ATP}}$ ), thus allowing an assessment of the energetic deficit relative to the known values of  $G_{\sim\text{ATP}}$  required for key cellular processes involved in excitation-contraction. The rate constants for ATP synthesis and the creatine kinase reaction were determined using magnetization transfer, allowing calculation of ATP and PCr fluxes. These observations, which include novel measurements of ATP synthesis,  $G_{\sim\text{ATP}}$  and [ADP] in MHD, provide the first direct

evidence that a deficit in ATP production causes a decrease in  $G_{-ATP}$  sufficient to impair the function of sarcoplasmic reticulum calcium ATPase (SERCA) in MHD, and may thus contribute to pump dysfunction.

## 2. Methods

### 2.1. Experimental animals

Male C57BL/6J mice 9 weeks of age were fed ad libitum either a control chow diet (Research Diets, product No. D09071703, 10% kcal lard, 0% sucrose) or a HFHS diet (Research Diets, product No. D09071702; 58% kcal lard, 13% kcal sucrose) for 4 months. The control diet (CD) was custom-formulated to match the micronutrients contained in the HFHS diet except for fat and sucrose. (Online Supplemental Table 1). We have previously reported increased body weight, increased fat mass, impaired glucose tolerance, fasting hyperglycemia and hyperinsulinemia as early as 8 weeks on the HFHS vs. CD diet [18]. The protocol was approved by the Institutional Animal Care and Use Committee of the Boston University School of Medicine.

### 2.2. Basal LV hemodynamic function in isolated perfused beating hearts

Left ventricular (LV) contractile function was assessed in an isolated retrograde-perfused Langendorff heart preparation in which the LV pressure/volume (PV) relationship was determined using the isovolumic, balloon-in-LV technique that allows assessment of LV function over a range of volumes that are normalized to heart weight [15]. Mice were heparinized (100 U IP) and anesthetized with sodium pentobarbital (150 mg/kg IP). The heart was excised, paced at a rate of 450 beats per minute (bpm) and perfused at a constant pressure of 80 mm Hg. The perfusate consisted of the following (in mmol/L): NaCl 118, NaHCO<sub>3</sub> 25, KCl 5.3, CaCl<sub>2</sub> 2, MgSO<sub>4</sub> 1.2, EDTA 0.5, glucose 10, pyruvate 0.5 equilibrated with 95% O<sub>2</sub> and 5% CO<sub>2</sub> (pH 7.4). A water-filled balloon was inserted into the LV for measurement of LV pressure and adjustment of LV volume. LV developed pressure (DevP) was determined (DevP = systolic pressure – end diastolic pressure). After stabilization for 20 min, the LV pressure/volume (PV) relationship was obtained by increasing the balloon volume in 5  $\mu$ L increments until the maximum DevP was achieved for each heart [15]. PV curves were determined under basal conditions (450 bpm, 2 mM Ca<sup>2+</sup>). These experiments were performed outside the NMR spectrometer using higher fidelity hemodynamic measurements in order to optimize the assessment of end-diastolic pressures.

### 2.3. Simultaneous measurement of LV contractile function and high energy phosphates by <sup>31</sup>P nuclear magnetic resonance (NMR) spectroscopy

In all subsequent studies, contractile function and high energy phosphates were measured simultaneously. Hearts were isolated as above and the perfusate was supplemented with glucose (10 mM) and pyruvate (0.5 mM) as energy substrates. In a separate subgroup of experiments, the perfusion buffer was supplemented with mixed long-chain fatty acids bound to 1% albumin resulting in the following concentrations (in mmol/L): palmitic acid (0.21), palmitoleic acid (0.04), linoleic acid (0.04), oleic acid (0.12), glucose (10) and insulin (50  $\mu$ U/mL) [16]. Perfused hearts were placed in a 9.4-Tesla superconducting magnet and maintained at 37 °C throughout the protocol. After stabilization, balloon volume was

adjusted to achieve an end-diastolic pressure of 8 to 9 mm Hg, and was held constant for the rest of the protocol. LV workload was changed by increasing the concentration of  $\text{CaCl}_2$  in the perfusate from 2 to 4 mM [16], increasing the pacing rate from 450 bpm to 600 bpm, or both. Heart rates (HR) of 450 and 600 bpm represent resting and high level of exercise (running at 21 m/s) of a C57BL/6 mouse, respectively [19]. Workload was estimated as the rate  $\times$  pressure product ( $\text{RPP} = \text{DevP} \times \text{HR}$ ) [16].

High energy phosphates were measured by  $^{31}\text{P}$  NMR spectroscopy (161.4 MHz, 9.4 T) using a Varian VNMRs spectrometer, as we have described [16,17,20]. NMR spectra were collected for 16 min at each level of work. Each  $^{31}\text{P}$  NMR spectrum resulted from the average of 208 free induction decay signals over 8 min. A reference capillary with an external standard (phenylphosphonic acid) was placed in the NMR tube next to the isolated heart to allow calculation of absolute concentrations of phosphocreatine (PCr), inorganic phosphate ( $\text{P}_i$ ) and ATP [17,20]. Saturation factors for all resonances were determined from fully relaxed spectra acquired with a recycle time of 20 s. Intracellular pH was calculated from the chemical shift of intracellular  $\text{P}_i$  relative to PCr [17,20]. At the end of each experiment, hearts were freeze clamped using Wollenberger tongs pre-cooled in liquid nitrogen and stored at  $-80^\circ\text{C}$  for subsequent analyses.

#### 2.4. Magnetization transfer experiments

In separate hearts, ATP synthesis and the forward CK reaction rates were measured with the 2-site saturation transfer technique by applying a low-power narrow-band radiofrequency pulse to saturate  $\gamma$ -ATP resonance and measure changes in the PCr and  $\text{P}_i$  resonance areas [16,21]. These measurements were performed at baseline workload (hearts paced at 450 bpm, 2 mM  $[\text{Ca}^{2+}]$  in the perfusate). Spectra were acquired without ( $M_0$ ) and with 4.8 s ( $M_\infty$ ) application of the selective saturating pulse. Each spectrum resulted from averaging a total of 256 scans, interleaved between sets of 8  $M_0$  and  $M_\infty$  scans. The  $M_0$  and  $M_\infty$  measurements were acquired in 44 min. The unidirectional pseudo-first-order rate constant of ATP synthesis was calculated as  $k_f = (M_0/M_\infty)/T_1 M_\infty$  and flux =  $k_f [\text{P}_i]$ , where  $T_1$  is the intrinsic longitudinal relaxation time for  $\text{P}_i$ ,  $[\text{P}_i]$  and  $M_0$  and  $M_\infty$  are magnetizations of  $\text{P}_i$  at 0 and 4.8 s, respectively. Similarly, for CK forward reaction, the unidirectional pseudo-first order rate constant  $k_f = (M_0/M_\infty)/T_1 M_\infty$  and flux =  $k_f [\text{PCr}]$ , where  $T_1$  is the intrinsic longitudinal relaxation time for PCr and  $M_0$  and  $M_\infty$  are magnetizations of PCr at 0 and 4.8 s, respectively.

#### 2.5. Calculation of the free energy of ATP hydrolysis ( $G_{\text{-ATP}}$ )

Total creatine concentration  $[\text{Cr}_{\text{total}}]$  was determined in heart samples by thin layer chromatography [22]. Tissue water content was assayed by drying a tissue powder aliquot 24 h at  $100^\circ\text{C}$ . The cytosolic creatine concentration ( $[\text{Cr}]$ ) was calculated as the difference between  $[\text{Cr}_{\text{total}}]$  and  $[\text{PCr}]$  measured by  $^{31}\text{P}$  NMR. Despite performing the  $^{31}\text{P}$  NMR spectroscopy ex vivo, free  $[\text{ADP}]$  could not be measured by  $^{31}\text{P}$  NMR directly [23]. Thus, free  $[\text{ADP}]$  was calculated using the creatine kinase reaction (Eq. (1)), which was assumed to be at equilibrium and where  $K_{\text{eq}} = 1.66 \times 10^9 \text{ M}^{-1}$  [24]:

$$[\text{ADP}] = ([\text{ATP}][\text{Cr}]) / ([\text{PCr}][\text{H}^+]) K_{\text{eq}} \quad (1)$$

The energy available in [ATP] for chemical work is expressed by the free energy of ATP hydrolysis ( $G_{\sim\text{ATP}}$ ), which is calculated by Eq. (2), where  $G^0$  ( $-30.5$  kJ/mol) is the value of  $G_{\sim\text{ATP}}$  under standard conditions of molarity, temperature, pH and  $[\text{Mg}^{2+}]$ ,  $R = 8.314$  J/mol·K, and  $T = 310$  K [24].

$$|\Delta G_{\sim\text{ATP}}| (\text{kJ/mol}) = |\Delta G^0 + RT \ln[\text{ADP}][\text{P}_i]/[\text{ATP}]| \quad (2)$$

The value of  $G_{\sim\text{ATP}}$  is negative, which denotes that the reaction is exergonic or energy-releasing. For the sake of clarity, we use the absolute value of  $G_{\sim\text{ATP}}$ ,  $|G_{\sim\text{ATP}}|$ .

## 2.6. Creatine kinase (CK) activity and protein expression

Total maximal CK activity was measured using a colorimetric Creatine Kinase Assay Kit according to the manufacturer's protocol (Abcam, Cambridge, MA) [25]. Briefly, freshly isolated tissue was homogenized in assay buffer, centrifuged to remove insoluble material, and supernatant was used for activity and immunoblotting. Protein concentration in the supernatant was determined by bicinchoninic acid assay (Pierce). Diluted supernatant (70–140 ng) was combined with ATP, CK Substrate, CK Enzyme Mix and CK Developer in a 96 well plate in duplicate, and color development was read at OD 450 nm for 30 min. Standards of NADH dilutions had the same mix without sample. Data is reported as the U/mg/min, where 1 U is the amount of CK that generates 1  $\mu\text{mol}$  NADH per minute.

CK immunoblots were performed using the identical supernatants. Protein (20  $\mu\text{g}$ ) was separated by SDS-PAGE, transferred to a PVDF membrane, and probed with rabbit anti-CK (Abcam) and mouse anti-GAPDH (Abcam) antibodies. Bands were visualized with IRDye<sup>®</sup> 800CW Donkey anti-Rabbit IgG and IRDye<sup>®</sup> 680LT Donkey anti-Mouse IgG (Licor), and fluorescent intensity was analyzed using a Licor Odyssey system. Data is reported as CK/GAPDH.

## 2.7. Statistical analysis

Results are presented as mean  $\pm$  SEM. Comparisons between groups were performed using unpaired *t*-tests, Mann-Whitney non-parametric tests or 2-way or repeated measures ANOVA, as appropriate. All statistical analyses were performed using GraphPad Prism software. P-value  $< 0.05$  was considered significant.

## 3. Results

### 3.1. Body and heart weight

All studies were performed after 4 months on either the HFHS or control (CD) diet, at which time the average age was  $27 \pm 1$  weeks. Body weight, heart weight and heart weight normalized to tibia length were increased in HFHS group. The daily caloric intake was approximately 11% higher in HFHS group (Table 1). We previously showed that 4 months

of HFHS diet leads to LV hypertrophy and diastolic dysfunction as assessed by trans-mitral and tissue Doppler echocardiography [10,11]. HFHS-fed mice recapitulate many aspects of the metabolic syndrome, including insulin resistance, increased plasma triglycerides and hypertension, making them an excellent model to study obesity-linked cardiovascular complications [18].

### 3.2. Basal contractile function

Basal function was determined with pacing at 450 bpm and a perfusate  $[Ca^{2+}]$  of 2 mM. In hearts from HFHS-fed (vs. CD-fed) mice the end-diastolic pressure was elevated over the entire range of LV volumes tested (Fig. 1A), indicative of impaired LV filling. In hearts from HFHS-fed (vs. CD-fed) mice LV systolic pressure was higher at low volumes, but was similar at the highest LV volumes tested (Fig. 1B). The maximal developed pressure (DevP) achieved was similar in HFHS and CD hearts (Fig. 1C), and likewise, LV DevP vs. EDP was identical for HFHS vs. CD hearts over the entire range of LV volumes tested (Fig. 1D). Thus, under basal conditions HFHS feeding led to diastolic dysfunction with preservation of systolic function confirming our prior echocardiographic findings [10,11] and showing that this isolated heart preparation exhibits hemodynamic features consistent with MHD.

### 3.3. Impaired contractile response to increased work

In a separate set of hearts, we next evaluated LV function and energetics simultaneously over a range of workloads. For these experiments, the LV balloon volume was set to achieve an LV end-diastolic pressure (LVEDP) of 8–9 mm Hg under basal conditions (pacing = 450 bpm, perfusate  $[Ca^{2+}] = 2$  mM). Work demand was raised incrementally by increasing the pacing rate from 450 to 600 bpm and increasing perfusate calcium from 2 to 4 mM, separately and in combination.

By design, LVEDP was identical in the HFHS and CD hearts under baseline conditions, but increased more in HFHS hearts at each higher level of work demand (Fig. 2A). At the highest work demand, LVEDP was  $25 \pm 2.3$  mm Hg in HFHS hearts vs.  $13.9 \pm 2.1$  mm Hg in CD hearts ( $p < 0.01$ ). In hearts from CD-fed mice, end-systolic pressure (Fig. 2B), developed pressure (Fig. 2C), and the RPP (Fig. 2D) increased progressively with higher work levels, whereas in HFHS hearts these increases were markedly blunted, indicative of a decrease in cardiac contractile reserve.

To ensure that substrate availability is not responsible for the observed differences in contractile function we perfused hearts with mixed long-chain fatty acids and insulin in addition to the regular Krebs-Henseleit (KH) buffer. Supplementation of the perfusate with mixed long-chain fatty acids and insulin had no effect on the observed differences in contractile response to high work demand (Supplemental Fig. 1).

### 3.4. Decreased high energy phosphate concentrations at baseline and with increasing workload

Concurrent with hemodynamic measurements, the concentrations of high-energy phosphates [PCr] and [ATP] were measured using  $^{31}P$  NMR spectroscopy. The ATP concentration was similar in hearts from HFHS- and CD-fed mice at baseline and all levels of work demand

(Fig. 3A). As expected [16,17], in hearts from CD-fed mice [PCr] and PCr/ATP decreased progressively with increasing work demand (Fig. 3B-C). In hearts from HFHS-fed mice, both [PCr] and the PCr/ATP ratio were lower at baseline and across all levels of work demand (Fig. 3B-C). Total [Cr] measured at the end of the study was the same for CD and HFHS hearts (Supplemental Fig. 2A). Intracellular pH (Supplemental Fig. 2B) and inorganic phosphate (Supplemental Fig. 2C) were also the same for both groups at all work levels. In contrast, cytosolic free [ADP], calculated as per Eq. (1), was higher in HFHS hearts at baseline and at all levels of work demand (Fig. 3D).

Supplementation of the perfusate with mixed long-chain fatty acids (LCFA) and insulin had no effect on [ATP], [PCr], the PCr/ATP ratio or cytosolic free [ADP] measured in CD or HFHS hearts at baseline or with any workload (Supplemental Fig. 3 A–D).

### 3.5. Free energy of ATP hydrolysis ( $G_{\sim\text{ATP}}$ )

The absolute value of free energy of ATP hydrolysis  $|G_{\sim\text{ATP}}|$  was lower in HFHS hearts at baseline and at all levels of increased work demand (Fig. 3E). Of note, at higher levels of work demand  $|G_{\sim\text{ATP}}|$  in HFHS hearts fell below 52 kJ/mol, the free energy required for normal function of sarcoplasmic reticulum ATPase (SERCA) [17,26,27]. Supplementation of the perfusate with mixed LCFA and insulin did not affect  $|G_{\sim\text{ATP}}|$  (Supplemental Fig. 3E).

### 3.6. High energy phosphate fluxes

To assess ATP synthesis in the intact beating heart, ATP synthesis and the forward CK reaction rates were measured using the  $^{31}\text{P}$  NMR transfer technique [16,21]. The pseudo-first order rate constant for ATP synthesis was decreased by 64% in HFHS vs. CD hearts (Fig. 4A), and flux through the ATP reaction, which reflects the production of ATP, was decreased by 34% in HFHS hearts (Fig. 4B). In HFHS hearts, the pseudo-first order rate constant for  $\text{CK}_{\text{forward}}$  was modestly increased (29%), and flux through  $\text{CK}_{\text{forward}}$  (the product of the rate constant and [PCr]) was unchanged (Fig. 4C and D).

### 3.7. CK protein expression and activity

CK protein expression assessed by immunoblotting was unchanged (vs. CD) in HFHS hearts (Supplemental Fig. 4), as was total CK activity (Supplemental Fig. 5).

## 4. Discussion

We used a mouse model of diet-induced MHD characterized by hemodynamic dysfunction to determine the relationship between energetics and pump function over a range of work demands in the isolated beating heart. Myocardial energetics were assessed using NMR spectroscopy to determine the concentrations of high energy phosphates, and magnetization transfer was used to determine flux through the ATP and CK reactions. In addition, for the first time in a beating heart model of MHD, we determined the free energy of ATP hydrolysis ( $G_{\sim\text{ATP}}$ ). There are several new findings. First,  $G_{\sim\text{ATP}}$  is decreased in MHD to an extent sufficient to limit the activity of SERCA. Second, the rate of ATP synthesis is decreased, while [ATP] is preserved and [ADP] is increased. Third, although [PCr] is

decreased, the CK forward rate constant is increased, CK activity and total creatine are normal, and the flux through CK is preserved. It is noteworthy that several of these findings differ from dilated cardiomyopathy, where the energy deficiency is associated with decreases in CK activity and flux, or have not been studied (e.g., ATP flux).

#### 4.1. Diastolic dysfunction at low work demand

Under low work conditions (450 bpm, corresponding to resting mouse heart rate [19], and a normal  $\text{Ca}^{2+}$  concentration) there was clear evidence of diastolic dysfunction in the HFHS hearts as reflected by higher LV end-diastolic pressures over a range of LV volumes. This was evident even at low LV volumes well within the physiologic range of LVEDP of 0–35 mm Hg. We previously showed that HFHS feeding for 4 months led to diastolic dysfunction in mice in vivo as reflected by abnormal LV filling and slowed LV relaxation measured by Doppler echocardiography [10]. The current ex vivo finding of impaired diastolic function in the isolated beating heart is consistent with our prior in vivo echocardiographic findings, showing that the diastolic dysfunction we observed in the isolated beating heart is of physiologic relevance.

Under low work conditions systolic function was preserved in HFHS hearts as evidenced by maximal LV end-systolic and developed pressures that were comparable to CD hearts over a wide range of LV volumes. Of note, the relationship between DevP and EDP (Fig. 1D) is nearly identical for HFHS and CD hearts over the entire LV volume range, further indicating that myocardial systolic function is preserved when the work demand is low.

#### 4.2. Decreased contractile reserve with increased work demand

In CD hearts, increasing the work demand led to a progressive increase in contractile function. In HFHS hearts the expected increases in ESP, DevP and RPP were all markedly depressed across the range of work levels. Thus, an increase in work demand revealed a marked impairment in the contractile reserve in HFHS hearts as evidenced by failure to increase systolic function despite an excessive increase in diastolic filling pressure. These results are similar to the lack of contractile reserve observed in patients with HFpEF [6,28,29], a clinical syndrome that is frequently caused by MHD.

#### 4.3. [PCr] is decreased in HFHS hearts

We found that myocardial [PCr] was markedly depressed in HFHS (vs. CD) hearts at all work levels. [PCr] and the [PCr]/[ATP] ratio are decreased in animal models of systolic heart failure [30–32] and humans with systolic failure due to dilated cardiomyopathy [32,33]. More limited data suggest that [PCr] is also decreased in animals [34] and humans with MHD due to type 2 diabetes [35] or obesity [8]. The functional importance of a decrease in [PCr] has been linked to a thermodynamic limitation for  $\text{Ca}^{2+}$  handling [24,27]. A decrease in the PCr/ATP ratio predicts mortality in patients with dilated cardiomyopathy [33], and correlates with diastolic dysfunction in patients with obesity [8].

#### 4.4. [ATP] is preserved and [ADP] is increased in HFHS hearts

[ATP] was normal in the HFHS hearts. Given the observed decrease in PCr, this finding was perhaps surprising, and differs from some studies in dilated CMP in which [ATP] was



shown to be decreased [36,37]. However, [ATP] is normal in other studies in dilated CMP [30], the disparity likely reflecting the severity of myocardial failure [31]. As predicted by the creatine kinase equilibrium equation (Eq. (1)), the observed decrease in [PCr]/[ATP] was associated with marked elevation in free [ADP] (Fig. 3D). In dilated cardiomyopathy there is depletion of total creatine [38,39], which may help to preserve normal [ADP] and  $|G_{\sim\text{ATP}}|$  [36]. In contrast to dilated cardiomyopathy, [total creatine] was normal in HFHS hearts (Supplemental Fig. 2A). An increase in [ADP] may contribute to the observed diastolic dysfunction, as failure to maintain a low [ADP] has been shown to impair diastolic dysfunction in hypertrophied myocardium [40]. To our knowledge, this is the first determination of [ADP] in animals or humans with MHD.

#### 4.5. The free energy of ATP hydrolysis ( $G_{\sim\text{ATP}}$ ) is decreased in HFHS hearts

It has been assumed that a decrease in [PCr] reflects a state of “energy starvation” in patients and animal models of dilated cardiomyopathy/systolic heart failure [31,32]. Likewise, [PCr] is decreased in MHD, suggesting that an energy deficiency also exists in MHD [10,12,34,41]. However, it is not known whether the energy deficit in MHD, as reflected by a decrease in [PCr], is sufficient to contribute to pump dysfunction. This question is further raised by our finding that [ATP] is normal in HFHS hearts. To address this important issue, we determined the free energy available for ATP hydrolysis ( $G_{\sim\text{ATP}}$ ), which is the driving force that powers cellular ATP-requiring processes.

In HFHS hearts  $|G_{\sim\text{ATP}}|$  was lower at baseline (relative to CD hearts). In addition,  $|G_{\sim\text{ATP}}|$  decreased progressively as work demand increased (see Fig. 4E) [26,27,39]. In the heart,  $|G_{\sim\text{ATP}}|$  is estimated to be 54–60 kJ/mol [26], which is adequate to support the  $|G_{\sim\text{ATP}}|$  requirements for proper function of the major myocyte ATPase reactions including sarcoplasmic reticulum  $\text{Ca}^{2+}$ -ATPase (SERCA; 52–53 kJ/mol),  $\text{Na}^{+}$ - $\text{K}^{+}$ -ATPase (48 kJ/mol), and actomyosin ATPase (45–50 kJ/mol) [26]. Of particular note, with increased work demand  $|G_{\sim\text{ATP}}|$  decreased below the value of 52 kJ/mol that is thought to be critical for support of the normal function of SERCA, an enzyme that is particularly susceptible to even modest decreases in  $G_{\sim\text{ATP}}$  [17,26,27]. Myocardial relaxation is highly ATP dependent [40], as the reuptake of calcium into the sarcoplasmic reticulum by SERCA is exquisitely sensitive to ATP depletion [17,26,27,39]. Adequate SERCA function is also critical to replenishing SR calcium stores that are required for normal systolic function. When  $|G_{\sim\text{ATP}}|$  is decreased by pharmacologic methods the hemodynamic consequences are similar to those we observed in HFHS-fed hearts, with diastolic dysfunction at baseline [42] and impaired contractile reserve at higher workloads [24]. To our knowledge, this is the first measurement of  $G_{\sim\text{ATP}}$  in a model of MHD.

#### 4.6. ATP flux (synthesis) is decreased in HFHS hearts

It is important to note that the concentrations of high energy phosphates [ATP], [ADP], [PCr] as well as the  $|G_{\sim\text{ATP}}|$  describe the thermodynamic status of the heart and reflect the relationship between the ATP synthesis and demand i.e. high energy phosphate kinetics. Thus, to further elucidate the mechanism responsible for the decrease in  $|G_{\sim\text{ATP}}|$ , we used magnetization transfer studies to determine the ATP synthesis rate constant and the flux of ATP. These experiments showed that, even under low work demand, both the rate constant

ATP synthesis ( $\text{ADP} + \text{P}_i \rightarrow \text{ATP}$ ) and ATP flux were depressed in HFHS hearts. These results indicate an impairment in ATP synthesis in HFHS-fed hearts. This finding has been suggested by prior observations based on indirect methods, e.g. oxygen consumption [9,12] or in isolated mitochondria [10,11]. The current study provides the first direct demonstration that ATP synthesis, per se, is decreased in MHD.

That the concentration of ATP is maintained in HFHS hearts, despite a decrease in ATP synthesis, indicates that ATP utilization must also be decreased. A decrease in ATP utilization may reflect ATPase inhibition by an elevated [ADP] that is known to occur [43]. Alternatively, or in addition, we cannot exclude the possibility that ATPase's are inhibited by other factors such as oxidative modifications. In either case, the observed decrease in ATPase activity may help to preserve [ATP] in the face of a decrease in synthesis, albeit, at the expense of a decrease in myocyte work performed [39]. Importantly, our findings are consistent with previously published in vivo studies from normal [44] and hypertrophied hearts [45,46].

#### 4.7. CK flux is preserved in HFHS hearts

In contrast to the observed decrease in ATP synthesis in HFHS-fed hearts, we found that the forward rate constant for CK ( $\text{CK}_{\text{forward}}$ ), CK flux, CK protein expression and total CK activity measured biochemically were all preserved in HFHS hearts. Taken together, these observations suggest that impaired CK function is not responsible for the observed decrease in [PCr].

While decreased CK activity has been observed in systolic heart failure [31,32] and hypertrophic cardiomyopathy [47], relatively little is known about CK function in MHD. Of note, our findings are consistent with those of Bashir et al. [34], who likewise found that the forward CK reaction rate constant was higher and CK flux was preserved in hearts from diabetic Zucker Diabetic Fatty (ZDF) rats. Taken together with the findings in the ZDF rat, our data suggest that a decrease in CK activity is not a major driver of cardiac energetic deficiency in the cardiomyopathy of MHD, but rather, support the thesis proposed by Bashir et al. [34] that the increase in the CK rate constant is a compensatory response that helps to maintain a normal flux through CK in the face of a decrease in [PCr] [34]. Interestingly, in other models of HFpEF such as pressure overload [48] and hypertrophic cardiomyopathy [47] CK flux is decreased, suggesting that the energetic profile in "HFpEF" may be heterogeneous and related to the underlying etiology.

#### 4.8. Creatine as "dispensable metabolite"

Important consideration is that creatine was somewhat controversially [49] shown to be a 'dispensable metabolite' in the heart [50]. In our study, we use the PCr/ATP ratio and creatine content to calculate ADP concentration and  $G_{\sim\text{ATP}}$ . If there were no creatine in the heart this approach would not be possible. A similar situation is present in the liver where there is no CK expression and thus no PCr. However, when CK was genetically introduced in the liver, ADP concentration measured by  $^{31}\text{P}$  NMR (PCr/ATP) was in agreement with biochemical measurements [51]. Thus, in the presence of a CK system, [PCr] is useful in assessing  $G_{\sim\text{ATP}}$ , the ultimate driving force for energy requiring processes in the cell [39].

#### 4.9. Potential limitations

Since our standard perfusion buffer is devoid of fatty acids, it was possible that the energetic deficit in HFHS hearts was a consequence of insufficient fatty acids in the buffer. Circulating fatty acids are an important source of energy for the healthy heart [52] and likely may take on increased importance in HFHS-fed hearts that have been exposed to increased fatty acids chronically [13,53]. However, supplementation of the perfusion buffer with mixed long chain fatty acids (LCFA) did not improve energetic or pump function in HFHS hearts, suggesting that under the conditions of these experiments the availability of exogenous LCFA is not limiting. We cannot exclude the possibility that the metabolic state caused by the HFHS diet leads to abnormalities in myocardial substrate utilization. Likewise, it is possible that the defects in mitochondrial function are independent of the metabolic substrate supplied [10,11]. In this study  $|G_{\sim ATP}|$  represents the average value across the heart and thus would not reflect potential local variations in the concentrations of high energy phosphates with regard to sarcoplasmic reticulum and other cellular micro-compartments.

#### 4.10. Clinical relevance

Obesity, type 2 diabetes and metabolic syndrome are strongly associated with the development of heart failure with preserved ejection fraction (HFpEF) [3-6]. While the integrated pathophysiology of HFpEF is complex and incompletely understood, it is clear that LV diastolic dysfunction is a major contributor [6,7,54]. Our observations indicate that impaired energy production may contribute to diastolic dysfunction in MHD. It is noteworthy that a decrease in the myocardial [PCr]/[ATP] ratio has been shown to correlate with the severity of impaired LV relaxation in patients with obesity-related heart disease [8,29]. These findings also suggest that impaired systolic function in this setting may only become evident when cardiac work is increased, thus emphasizing the importance of studying this pathophysiology under conditions of varying cardiac work. Clinically, in patients with HFpEF, exercise is an important precipitant of symptoms and elevated pulmonary artery pressures [6,28,55]. Likewise, symptoms and exercise intolerance correlate poorly with the degree of diastolic dysfunction assessed at rest [6]. Our findings suggest that the inability to increase cardiac work due to energetic limitations may be an important cause of exercise intolerance and symptoms in patients with HFpEF. Peripheral factors, some energetic, may contribute to exercise intolerance in HFpEF as well [56]. Thus, while we cannot exclude a role for other factors (e.g., increased myocardial stiffness due to fibrosis or altered properties/function of titin), therapeutic strategies to improve myocardial energetics may be of value in the treatment of HFpEF in the setting of MHD due to obesity, type 2 diabetes and/or metabolic syndrome (Table 2).

### Supplementary Material

Refer to Web version on PubMed Central for supplementary material.

### Acknowledgments

#### Funding source

Supported by NIH grants HL-064750 (WSC), EB 014414 (JAB), NIDDK R01 DK103750 (MMB) and the NHLBI-sponsored Boston University Cardiovascular Proteomics Center (Contract No. N01-HV-28178, WSC). Dr. Bachschmid was also funded by American Heart Association “Grant in Aid” 16GRNT27660006. Dr. Sverdlov was funded by a CJ Martin Fellowship (APP1037603) from the National Health and Medical Research Council of Australia, AHA Postdoctoral Fellowship (14POST20490003) and Future Leader Fellowship (Award ID 101918) from Heart Foundation of Australia. Dr. Luptak is the recipient of an AHA Fellow-to-Faculty Award 15FTF25890062.

## References

- Ogden CL, Carroll MD, Fryar CD, Flegal KM. Prevalence of obesity among adults and youth: United States, 2011–2014. *NCHS Data Brief*. 2015 ;1–8.
- Haffner S, Taegtmeier H. Epidemic obesity and the metabolic syndrome. *Circulation*. 108 2003; :1541–1545. [PubMed: 14517149]
- Ayalon N, Gopal DM, Mooney DM, Simonetti JS, Grossman JR, Dwivedi A, et al. Preclinical left ventricular diastolic dysfunction in metabolic syndrome. *Am J Cardiol*. 114 2014; :838–842. [PubMed: 25084691]
- De Las Fuentes L, Brown AL, Mathews SJ, Waggoner AD, Soto PF, Gropler RJ, et al. Metabolic syndrome is associated with abnormal left ventricular diastolic function independent of left ventricular mass. *Eur Heart J*. 28 2007; :553–559. [PubMed: 17311827]
- Fontes-Carvalho R, Ladeiras-Lopes R, Bettencourt P, Leite-Moreira A, Azevedo A. Diastolic dysfunction in the diabetic continuum: association with insulin resistance, metabolic syndrome and type 2 diabetes. *Cardiovasc Diabetol*. 14 2015; :4–13. [PubMed: 25582424]
- Borlaug BA. The pathophysiology of heart failure with preserved ejection fraction. *Nat Rev Cardiol*. 11 2014; :507–515. [PubMed: 24958077]
- Sharma K, Kass DA. Heart failure with preserved ejection fraction: mechanisms, clinical features, and therapies. *Circ Res*. 115 2014; :79–96. [PubMed: 24951759]
- Rider OJ, Francis JM, Ali MK, Holloway C, Pegg T, Robson MD, et al. Effects of catecholamine stress on diastolic function and myocardial energetics in obesity. *Circulation*. 125 2012; :1511–1519. [PubMed: 22368152]
- Mazumder PK, Neill BTO, Roberts MW, Buchanan J, Yun UJ, Cooksey RC, et al. Impaired cardiac efficiency and increased fatty acid oxidation in insulin-resistant ob/ob mouse hearts. *Diabetes*. 53 2004; :2366–2374. [PubMed: 15331547]
- Sverdlov AL, Elezaby A, Qin F, Behring JB, Luptak I, Calamaras TD, et al. Mitochondrial reactive oxygen species mediate cardiac structural, functional, and mitochondrial consequences of diet-induced metabolic heart disease. *J Am Heart Assoc*. 5 2016; :1–13.
- Sverdlov AL, Elezaby A, Behring JB, Bachschmid MM, Luptak I, Tu VH, et al. High fat, high sucrose diet causes cardiac mitochondrial dysfunction due in part to oxidative post-translational modification of mitochondrial complex II. *J Mol Cell Cardiol*. 78 2015; :165–173. [PubMed: 25109264]
- Boudina S, Sena S, Theobald H, Sheng X, Wright JJ, Hu XX, et al. Mitochondrial energetics in the heart in obesity-related diabetes: direct evidence for increased uncoupled respiration and activation of uncoupling proteins. *Diabetes* 2007. Jul 12. 2007 :2457–2466.
- Bugger H, Abel ED. Molecular mechanisms for myocardial mitochondrial dysfunction in the metabolic syndrome. *Clin Sci (Lond)*. 114 2008; :195–210. [PubMed: 18184113]
- Qin F, Siwik DA, Luptak I, Hou X, Wang L, Higuchi A, et al. The polyphenols resveratrol and S17834 prevent the structural and functional sequelae of diet-induced metabolic heart disease in mice. *Circulation*. 125 2012; :1756–1757.
- Luptak I, Yan J, Cui L, Jain M, Liao R, Tian R. Long-term effects of increased glucose entry on mouse hearts during normal aging and ischemic stress. *Circulation*. 116 2007; :901–909. [PubMed: 17679614]
- Luptak I, Balschi JA, Xing Y, Leone TC, Kelly DP, Tian R. Decreased contractile and metabolic reserve in peroxisome proliferator-activated receptor- $\alpha$ -null hearts can be rescued by increasing glucose transport and utilization. *Circulation*. 112 2005; :2339–2346. [PubMed: 16203912]

17. Pinz I, Tian R, Belke D, Swanson E, Dillmann W, Ingwall JS. Compromised myocardial energetics in hypertrophied mouse hearts diminish the beneficial effect of overexpressing SERCA2a. *J Biol Chem.* 286 2011; :10163–10168. [PubMed: 21278384]
18. Weisbrod RM, Shiang T, Al SL, Fry JL, Bajpai S, Reinhart-King CA, et al. Arterial stiffening precedes systolic hypertension in diet-induced obesity. *Hypertension.* 62 2013; :1105–1110. [PubMed: 24060894]
19. Andreev-Andrievskiy AA, Popova AS, Borovik AS, Dolgov ON, Tsvirkun DV, Custaud M, et al. Stress-associated cardiovascular reaction masks heart rate dependence on physical load in mice. *Physiol Behav.* 132 2014; :1–9. [PubMed: 24802359]
20. Jansen MA, Shen H, Zhang L, Wolkowicz PE, Balschi JA. Energy requirements for the Na<sup>+</sup> gradient in the oxygenated isolated heart: effect of changing the free energy of ATP hydrolysis. *Am J Physiol Heart Circ Physiol.* 285 2003; :H2437–45. [PubMed: 12958035]
21. Bittl JA, Ingwall JS. Reaction rates of creatine kinase and ATP synthesis in the isolated rat heart. A <sup>31</sup>P NMR magnetization transfer study. *J Biol Chem.* 260 1985; :3512–3517. [PubMed: 3972835]
22. Kammermeier H. Microassay extracts of free and total of creatine. *Anal Biochem.* 345 1973; :341–345.
23. Balaban RS. The application of nuclear magnetic resonance to the study of cellular physiology. *Am J Phys Cell Phys.* 246 1985; :C10–C19.
24. Tian R, Ingwall JS. Energetic basis for reduced contractile reserve in isolated rat hearts. *Am J Phys Heart Circ Phys.* 270 1996; :H1207–H1216.
25. Cindrova-Davies T, Tissot Van Patot M, Gardner L, Jauniaux E, Burton GJ, Charnock-Jones DS. Energy status and HIF signalling in chorionic villi show no evidence of hypoxic stress during human early placental development. *Mol Hum Reprod.* 21 2014; :296–308. [PubMed: 25391298]
26. Kammermeier H. High energy phosphate of the myocardium: concentration versus free energy change. *Basic Res Cardiol.* 82 1987; :31–36. [PubMed: 2959262]
27. Tian R, Halow JM, Meyer M, Dillmann WH, Figueredo VM, Ingwall JS, et al. Thermodynamic limitation for Ca<sup>2+</sup> handling contributes to decreased contractile reserve in rat hearts. *Am J Physiol Heart Circ Physiol.* 275 1998; :H2064–71.
28. Abudiab MM, Redfield MM, Melenovsky V, Olson TP, Kass DA, Johnson BD, et al. Cardiac output response to exercise in relation to metabolic demand in heart failure with preserved ejection fraction. *Eur J Heart Fail.* 15 2013; :776–785. [PubMed: 23426022]
29. Phan TT, Abozguia K, Nallur SG, Mahadevan G, Ahmed I, Williams L, et al. Heart failure with preserved ejection fraction is characterized by dynamic impairment of active relaxation and contraction of the left ventricle on exercise and associated with myocardial energy deficiency. *J Am Coll Cardiol.* 54 2009; :402–409. [PubMed: 19628114]
30. Neubauer S, Horn M, Naumann A, Tian R, Hu K, Laser M, et al. Impairment of energy metabolism in intact residual myocardium of rat hearts with chronic myocardial infarction. *J Clin Investig.* 95 1995; :1092–1100. [PubMed: 7883957]
31. Ingwall JS, Weiss RG. Is the failing heart energy starved? On using chemical energy to support cardiac function. *Circ Res.* 95 2004; :135–145. [PubMed: 15271865]
32. Weiss RG, Gerstenblith G, Bottomley PA. ATP flux through creatine kinase in the normal, stressed, and failing human heart. *Proc Natl Acad Sci U S A.* 102 2005; :808–813. [PubMed: 15647364]
33. Neubauer S, Krahe T, Schindler R, Horn M, Hillenbrand H, Entzeroth C, et al. <sup>31</sup>P magnetic resonance spectroscopy in dilated cardiomyopathy and coronary artery disease. *Circulation.* 86 1992; :1810–1818. [PubMed: 1451253]
34. Bashir A, Coggan AR, Gropler RJ. In vivo creatine kinase reaction kinetics at rest and stress in type II diabetic rat heart. *Phys Rep.* 3 2015; :e12248.
35. Rijzewijk LJ, Jonker JT, Van Der Meer RW, Lubberink M, De Jong HW, Romijn JA, et al. Effects of hepatic triglyceride content on myocardial metabolism in type 2 diabetes. *J Am Coll Cardiol.* 56 2010; :225–233. [PubMed: 20620743]
36. Shen W, Vatner DE, Vatner SF, Ingwall JS. Progressive loss of creatine maintains a near normal deltaGATP in transgenic mouse hearts with cardiomyopathy caused by overexpressing Gsalpha. *J Mol Cell Cardiol.* 48 2010; :591–599. [PubMed: 19913550]

37. Liao R, Nascimben L, Friedrich J, Gwathmey JK, Ingwall JS. Decreased energy reserve in an animal model of dilated cardiomyopathy: relationship to contractile performance. *Circ Res.* 78 1996; :893–902. [PubMed: 8620610]
38. Nakae I, Mitsunami K, Omura T, Yabe T, Tsutamoto T, Matsuo S, et al. Proton magnetic resonance spectroscopy can detect creatine depletion associated with the progression of heart failure in cardiomyopathy. *J Am Coll Cardiol.* 42 2003; :1587–1593. [PubMed: 14607443]
39. Ingwall, JS. *ATP and the Heart*. Kluwer Academic Publishers; Dordrecht/Boston/London, Boston: 2002.
40. Tian R, Nascimben L, Ingwall JS, Lorell BH. Failure to maintain a low ADP concentration impairs diastolic function in hypertrophied rat hearts. *Circulation.* 96 1997; :1313–1319. [PubMed: 9286964]
41. Rider OJ, Francis JM, Tyler D, Byrne J, Clarke K, Neubauer S. Effects of weight loss on myocardial energetics and diastolic function in obesity. *Int J Card Imaging.* 29 2013; :1043–1050.
42. Tian R, Christie ME, Spindler M, Hopkins JCA, Halow JM, Camacho SA, et al. Role of MgADP in the development of diastolic dysfunction in the intact beating rat heart. *J Clin Investig.* 99 1997; :745–751. [PubMed: 9045879]
43. Atkinson DE. The Energy charge of the adenylate pool as a regulatory parameter. Interaction with feedback modifiers. *Biochemistry.* 7 1968; :4030–4034. [PubMed: 4972613]
44. Xiong Q, Du F, Zhu X, Zhang P, Suntharalingam P, Ippolito J, et al. ATP production rate via creatine kinase or ATP synthase in vivo: a novel superfast magnetization saturation transfer method. *Circ Res.* 108 2011; :653–663. [PubMed: 21293002]
45. Xiong Q, Zhang P, Guo J, Swingen C, Jang A, Zhang J. Myocardial ATP hydrolysis rates in vivo: a porcine model of pressure overload-induced hypertrophy. *Am J Physiol Heart Circ Physiol.* 309 2015; :H450–H458. [PubMed: 26024682]
46. Gong G, Liu J, Liang P, Guo T, Hu Q, Ochiai K, et al. Oxidative capacity in failing hearts. *Am J Physiol Heart Circ Physiol.* 285 2003; :H541–H548. [PubMed: 12714322]
47. Abraham MR, Bottomley PA, Dimaano VL, Pinheiro A, Steinberg A, Traill TA, et al. Creatine kinase adenosine triphosphate and phosphocreatine energy supply in a single kindred of patients with hypertrophic cardiomyopathy. *Am J Cardiol.* 112 2013; :861–866. [PubMed: 23751935]
48. Maslov MY, Chacko VP, Stuber M, Moens AL, Kass DA, Champion HC, et al. Altered high-energy phosphate metabolism predicts contractile dysfunction and subsequent ventricular remodeling in pressure-overload hypertrophy mice. *Am J Physiol Heart Circ Physiol.* 292 2007; :H387–91. [PubMed: 16963614]
49. Taegtmeyer H, Ingwall JS. Creatine-A dispensable metabolite? *Circ Res.* 112 2013; :878–880. [PubMed: 23493302]
50. Lygate CA, Aksentijevic D, Dawson D, Ten Hove M, Phillips D, De Bono JP, et al. Living without creatine: unchanged exercise capacity and response to chronic myocardial infarction in creatine-deficient mice. *Circ Res.* 112 2013; :945–955. [PubMed: 23325497]
51. Koretsky AP, Brosnan MJ, Chen LH, Chen JD, Van Dyke T. NMR detection of creatine kinase expressed in liver of transgenic mice: determination of free ADP levels. *Proceedings of the National Academy of Sciences of the United States of America.* 87 1990; :3112–3116. [PubMed: 2326269]
52. Saddik M, Lopaschuk GD. Myocardial triglyceride turnover and contribution to energy substrate utilization in isolated working rat hearts. *J Biol Chem.* 266 1991; :8162–8170. [PubMed: 1902472]
53. Wilson CR, Tran MK, Salazar KL, Young ME, Taegtmeyer H. Western diet, but not high fat diet, causes derangements of fatty acid metabolism and contractile dysfunction in the heart of Wistar rats. *Biochem J.* 406 2007; :457–467. [PubMed: 17550347]
54. Zile MR, Baicu CF, Ikonomidis JS, Stroud RE, Nietert PJ, Bradshaw AD, et al. Myocardial stiffness in patients with heart failure and a preserved ejection fraction: contributions of collagen and titin. *Circulation.* 131 2015; :1247–1259. [PubMed: 25637629]
55. Santos M, Opatowsky AR, Shah AM, Tracy J, Waxman AB, Systrom DM. Central cardiac limit to aerobic capacity in patients with exertional pulmonary venous hypertension: implications for heart failure with preserved ejection fraction. *Circulation.* 8 2015; :275–285.

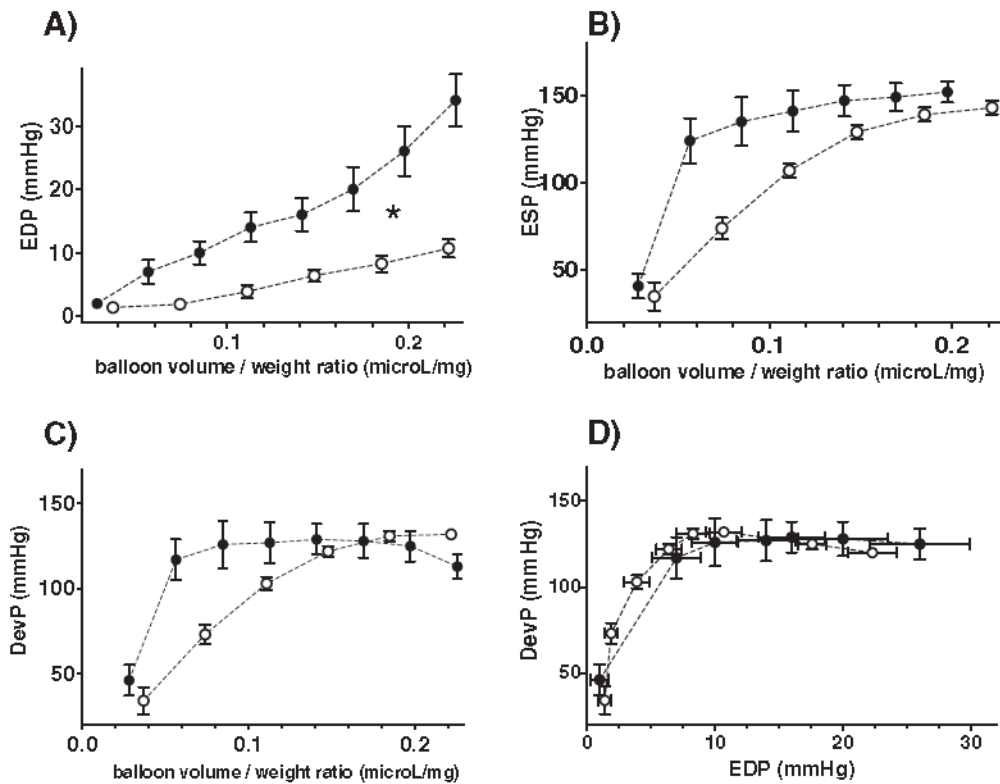
56. Weiss K, Schär M, Panjath GS, Zhang Y, Sharma K, Bottomley PA, et al. Fatigability, exercise intolerance, and abnormal skeletal muscle energetics in heart failure. *Circulation*. 10 2017;

Author Manuscript

Author Manuscript

Author Manuscript

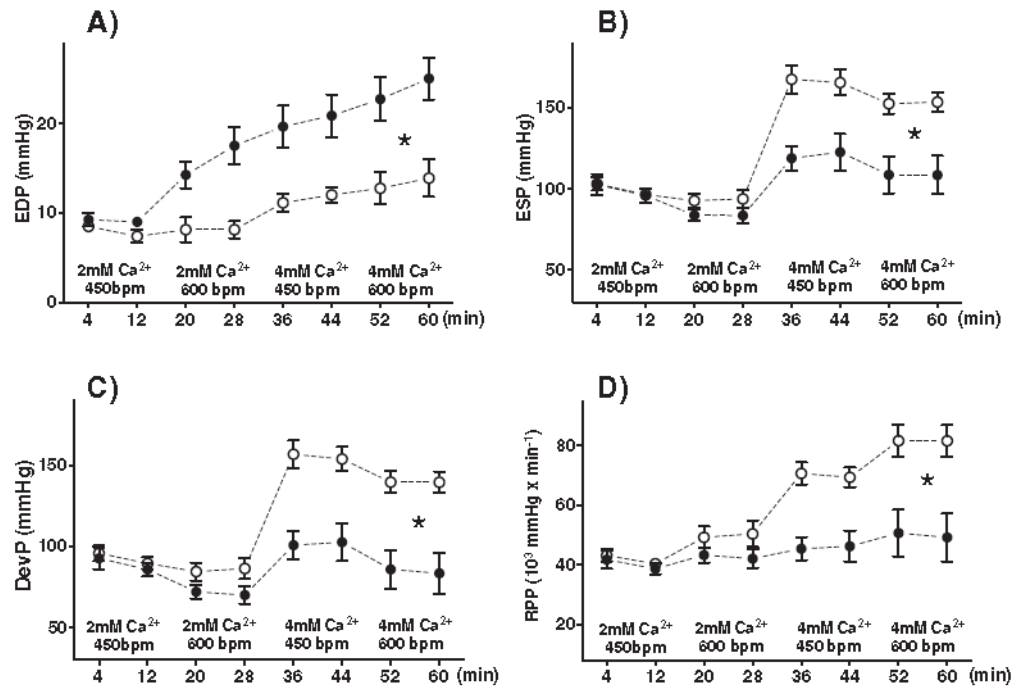
Author Manuscript



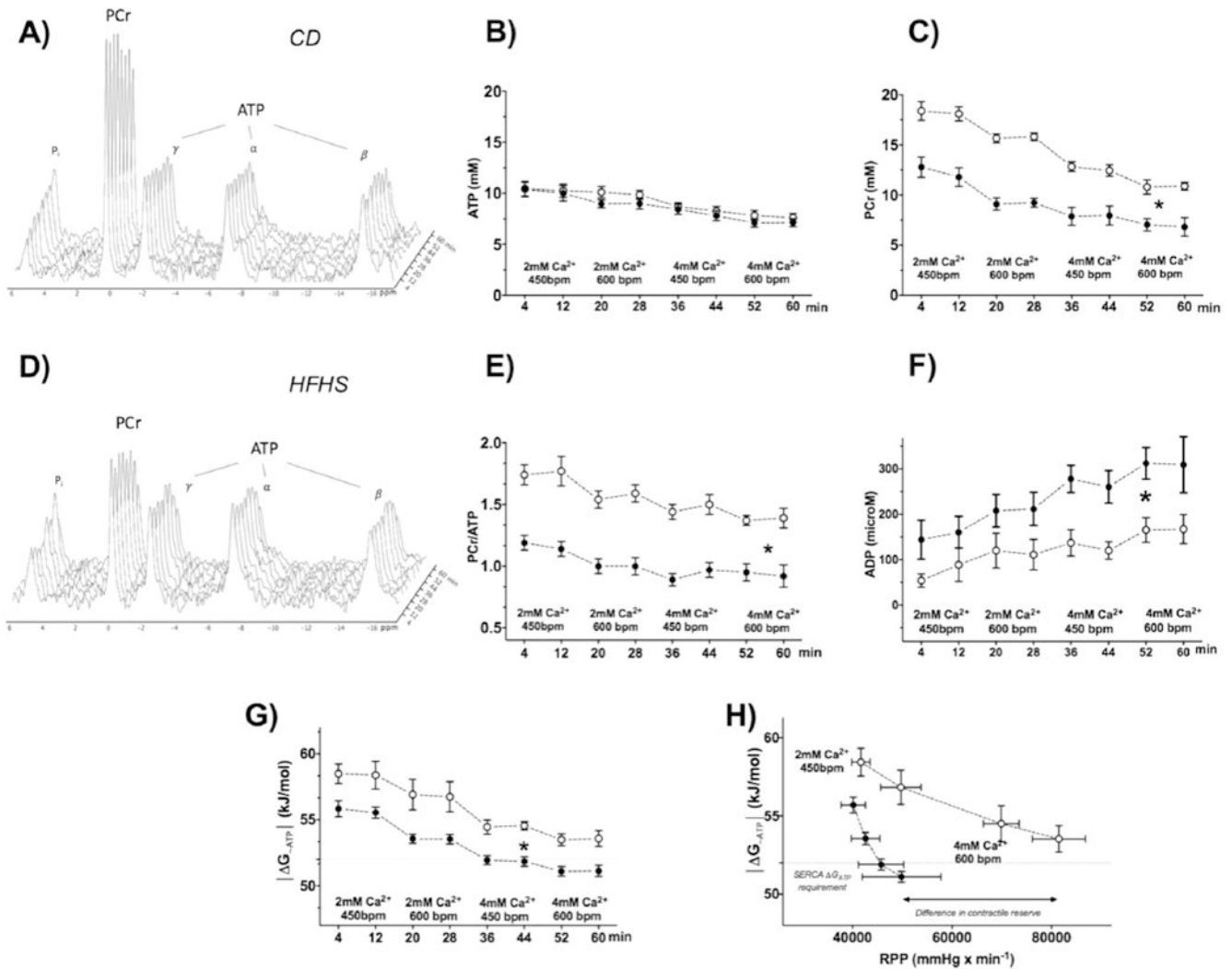
**Fig. 1.**

Diastolic function is impaired while contractile function is preserved in HFHS- vs. CD-fed hearts under low workload conditions. LV function was assessed by the isovolumic Langendorff method over a range of LV volumes while hearts were paced at 450 bpm. For any given LV volume, end-diastolic pressure (EDP) was higher in HFHS- vs. CD-fed mice, indicating diastolic dysfunction (Panel A). For HFHS-fed hearts the end-systolic pressure (ESP) - volume relationship was steeper (Panel B), but the maximal developed pressures (Panel C) and the relationship between developed pressure (DevP) and end-diastolic pressure (EDP) (Panel D) were similar to those in CD-fed hearts. For all panels data are shown as mean  $\pm$  SEM; open circles = CD-fed mice and filled circles = HFHS-fed mice; n = 8 in each group; \* = p < 0.05.



**Fig. 2.**

Contractile reserve is decreased in isolated perfused hearts from HFHS-fed mice. LV contractile function was assessed at 4 levels of progressively increasing myocardial work demand. Hearts were paced at heart rate (HR) 450 bpm at baseline, and paced at 600 bpm and/or Ca<sup>2+</sup> was raised (4 mM) to increase work demand and in competent hearts, contractile performance. With increased work demand, the LV end-diastolic pressure (EDP) increased more in hearts from HFHS-fed (vs. CD-fed) mice (Panel A). At baseline demand (2 mM Ca<sup>2+</sup>, 450 bpm), end-systolic pressure (ESP) (Panel B), developed pressure (DevP) (Panel C) and the rate x pressure product (RPP) (Panel D) were all similar in HFHS- and CD-fed hearts. However, with increased work demand all three measures failed to increase appropriately. For all panels data are shown as mean  $\pm$  SEM; open circles = CD-fed mice and filled circles = HFHS-fed mice; n = 8 in each group; \* = p < 0.05.

**Fig. 3.**

Energetic function is impaired in isolated perfused hearts from HFHS-fed mice. Concurrent with hemodynamic measurements at progressively increasing levels of work demand (Fig. 2), myocardial high energy phosphates were measured using  $^{31}\text{P}$  NMR spectroscopy. Stack of representative  $^{31}\text{P}$  NMR spectra at each stage of the protocol is shown in Panel A (CD) and Panel D (HFHS). ATP concentrations ( $[\text{ATP}]$ ) were similar in HFHS- and CD-fed hearts at all work demands (Panel B). However, in HFHS hearts the concentration of phosphocreatine (PCr; Panel C) and the PCr/ATP ratio (Panel E) were lower at baseline and at all workloads, reflecting an impairment in energy reserve. Calculated cytosolic free [ADP] was higher in HFHS- vs. CD-fed hearts at baseline and all increased workloads (Panel F). The energy available for chemical work in ATP is expressed by the free energy of ATP hydrolysis ( $G_{\text{ATP}}$ ). As  $G_{\text{ATP}}$  is a negative number due to the exergonic nature of ATP hydrolysis, the absolute value is depicted for the sake of clarity.  $|\Delta G_{\text{ATP}}|$  was lower in HFHS-fed hearts at baseline and all stages of work demand (Panel G). The lack of energy reserve in HFHS group is even better visualized when  $|\Delta G_{\text{ATP}}|$  is plotted against actual

work performed, RPP (Panel H). In panels G and H, the dotted horizontal line at a  $|G_{-ATP}|$  of 52 kJ/mol is the value required for normal function of sarcoplasmic reticulum ATP-ase. For all panels data are shown as mean  $\pm$  SEM; open circles = CD-fed mice and filled circles = HFHS-fed mice; n = 8 in each group; \* =  $p < 0.05$ .

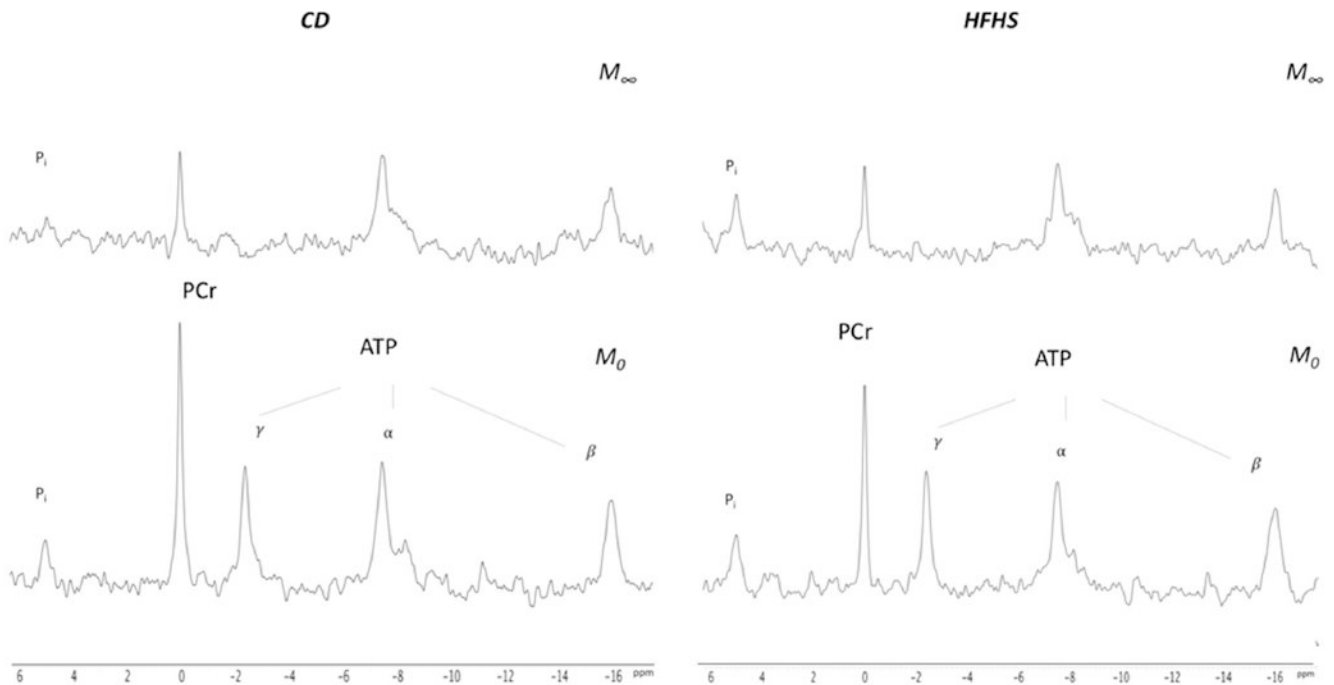


**Fig. 4.** Representative  $^{31}\text{P}$  NMR magnetization transfer spectra. Spectra were collected from CD and HFHS hearts at 0 s ( $M_0$ ) and 4.8 s ( $M_\infty$ ) after a saturating pulse was applied to  $\gamma$ -P of the ATP. The peaks are assigned (from left to right) as  $\text{P}_i$ , PCr,  $\gamma$ -ATP,  $\alpha$ -ATP and  $\beta$ -ATP. Note the disappearance of the  $\gamma$ -ATP peak (saturated) at  $M_\infty$ . The exchange of the saturated [ $\gamma$ -P] between ATP and  $\text{P}_i$  resulted in reduced  $\text{P}_i$  peak area (decrease is larger in CD heart than in HFHS heart reflecting higher rate of ATP synthesis). Similarly, the decrease in PCr peak area reflects the CK forward flux. These measurements were performed at baseline workload with 2 mM  $[\text{Ca}^{2+}]$  in the perfusate and paced at 450 bpm.

**Table 1**

## Body and organ weights.

|                                  | <b>CD</b>   | <b>HFHS</b>   |
|----------------------------------|-------------|---------------|
| Age, weeks                       | 27.1 ± 1.2  | 26.8 ± 1.1    |
| Body weight, g                   | 28.4 ± 4.0  | 49.1 ± 5.3 *  |
| Heart weight, mg                 | 112.2 ± 3.7 | 148.3 ± 6.5 * |
| Tibia length, mm                 | 17.5 ± 0.3  | 18.1 ± 0.3    |
| Heart weight/tibia length, mg/mm | 6.4 ± 0.5   | 8.2 ± 0.4 *   |
| Caloric intake, kcal/mouse/day   | 14.5 ± 0.3  | 16.2 ± 0.6 *  |

Values are mean ± SEM; n = 10 in each group.

\* P < 0.01.

Author Manuscript

Author Manuscript

Author Manuscript

Author Manuscript

**Table 2**<sup>31</sup>P NMR Magnetization transfer measurements.

|  | CD           | HFHS           |
|--|--------------|----------------|
| Rate constant for ATP synthesis (s <sup>-1</sup> ) | 0.274 ± 0.06 | 0.095 ± 0.01   |
| ATP synthesis rate (μmol/min/g w.w.)               | 29.8 ± 1.6   | 20.1 ± 2.84 *  |
| Rate constant for CK <sub>forward</sub>            | 0.139 ± 0.01 | 0.177 ± 0.01 * |
| CK <sub>forward</sub> flux (μmol/min/g w.w.)       | 62.1 ± 2.5   | 55.7 ± 2.6     |

The rate constant for ATP synthesis (ADP + Pi → ATP) and the flux through the reaction (rate constant × [Pi]) were lower in HFHS hearts. The pseudo first-order rate constant for CK<sub>forward</sub> (PCr + ADP → ATP + Cr) was increased in HFHS group. Flux through CK<sub>forward</sub> (rate constant × [PCr]) was unchanged (p = 0.21) in HFHS compared to CD hearts. Values are mean ± SEM; n = 4–7 in each group.

\* P < 0.05.